Jurnal ELTIKOM :
Jurnal Teknik Elektro, Teknologi Informasi dan Komputer

Vol. 9, No. 2, December 2025, page. 218-227
ISSN 2598-3245 (Print), ISSN 2598-3288 (Online)
DOI: http://doi.org/10.31961/eltikom.v9i2.1483
Available online at http://eltikom.poliban.ac.id

A VGG16 CNN-BASED METHOD FOR MULTICLASS LUNG CANCER CLASSIFICATION USING CT IMAGING

Sekar Sari[1*], Muna Afdi Muniroh[2], Kevin Ilham Apriandy[3]
[1)] Department of Electrical Technology, Politeknik Internasional Tamansiswa Mojokerto, Mojokerto, Indonesia
[2)] Department of Mathematics, Universitas PGRI Ronggolawe, Tuban, Indonesia
[3)] Department of Computer Technology, Politeknik Internasional Tamansiswa Mojokerto, Mojokerto, Indonesia
e-mail: sekarsari103@gmail.com, munaafdimuniroh@gmail.com, kevinapriandy@gmail.com

Received: 11 March 2025 – Revised: 28 May 2025 – Accepted: 4 June 2025

ABSTRACT

Lung cancer is the leading cause of death worldwide among all types of cancer. Early detection and accurate classification are essential to prevent disease progression and improve patient survival rates. One effective approach is the use of computer-aided diagnosis (CAD) systems based on medical imaging, particularly CT scans, which provide high-resolution and non-invasive visualization of lung structures, including blood vessels, soft tissues, and lesions or nodules. This study proposes a VGG16 CNN-based multiclass classification method for lung cancer. Unlike previous studies that primarily focus on binary classification, this research addresses four distinct classes of lung nodule CT images to better reflect complex clinical needs. The modified VGG16 architecture incorporates additional layers, including Flatten, Dense, and Dropout, along with the Softmax activation function, effectively improving classification performance and reducing overfitting risk. An ablation experiment was also conducted by replacing ReLU with LeakyReLU to address the potential "dying ReLU" issue. However, the results indicated that LeakyReLU did not provide significant improvement over the standard ReLU. The proposed model achieved an accuracy of 90.72%, precision of 91.5%, sensitivity of 89.25%, specificity of 96.76%, F1-score of 90%, and a low loss value of 0.37. Furthermore, the modified VGG16-CNN outperformed other CNN architectures, including ResNet50, EfficientNetB1, MobileNetV2, and AlexNet, in multiclass lung cancer image classification. The results demonstrate that the proposed method is effective for diagnosing lung nodules from CT scans and has the potential to support medical professionals in making accurate and timely diagnoses.

Keywords*: classification, CT imaging, lung cancer, modified VGG16-CNN.*

I. INTRODUCTION

LUNG cancer is a disease characterized by the uncontrolled growth of abnormal cells in the lungs, forming a mass or tumor. These cells originate from genetic mutations that disrupt normal lung function. Lung cancer remains the leading cause of death among all types of cancer [1] and ranks as the second most common cancer globally after breast cancer. According to data from the World Health Organization (WHO) in 2020, there were 28,633 cases of lung cancer in Indonesia in 2019. In 2022, the United States reported an estimated 1,918,030 new cancer cases and 609,360 deaths, with lung cancer accounting for the highest number of cancer-related deaths—approximately 350 per day [2]. Early detection of lung nodules significantly increases the success rate of treatment and improves patient survival outcomes.

A lung nodule is an abnormal growth that may appear in one or both lungs. These nodules can develop due to external factors such as smoking, infections, environmental exposure, and other harmful substances. They vary in size, shape, volume, and density [3], and multiple nodules may exist within the same lung. The analysis of lung nodules is crucial for the early prevention of lung cancer through accurate identification and classification. This classification can be performed using computer-aided diagnosis (CAD) systems that recognize images and extract regions of interest (ROI) from various imaging modalities [4]. CAD systems enhance the accuracy and efficiency of image detection and disease diagnosis, determine malignancy levels, and help reduce potential errors in detection.

The imaging modalities used in CAD systems for lung cancer include computed tomography (CT) [5], [6], X-ray [7]–[9], magnetic resonance imaging (MRI) [10], and positron emission tomography (PET) [11]. Among these, CT scans are considered one of the most effective tools for detecting lung cancer and analyzing nodules [12]. CT scan images provide high resolution, allowing for clear visualization of lung structures such as blood vessels, soft tissue, and bones, as well as the detection of lesions [1]. Moreover, CT imaging is a non-invasive procedure that does not require surgical incisions, making it a safer and more comfortable diagnostic option.

This study draws on several previous studies related to deep learning, particularly the Convolutional Neural Network (CNN), which has proven to be an effective automated method for detection, diagnosis, and optimization in medical imaging analysis. In lung nodule detection, CNNs have achieved remarkable results and significantly reduced false positive rates [13]. One widely used CNN architecture is VGG16, which consists of 16 layers [14]. Abraham et al. classified nodules and non-nodules in lung CT images using the AlexNet and VGG16 CNN architectures, both designed for early lung cancer prediction with the LIDC-IDRI dataset. Their tests showed that VGG16 outperformed AlexNet, achieving an accuracy of 97.5% [15]. Similarly, Akter et al. employed VGG16 to classify 2,861 lung X-ray images into two categories—pneumonia and normal—and compared its performance with Inception V3 and ResNet50. Among the three CNN architectures tested, VGG16 demonstrated the best performance, achieving 95% accuracy, 94% precision, 96.4% sensitivity, and 92.8% specificity [16].

Previous studies have generally used VGG16 for binary classification of lung images but rarely for multiclass classification. A hybrid CNN and SVM approach was previously used to classify lung cancer into four types—adenocarcinoma, large-carcinoma, normal, and squamous-carcinoma [17]—but limited research has applied the VGG16-CNN architecture to multiclass lung cancer classification. Nonetheless, existing studies indicate that VGG16-CNN has strong potential for effective classification of lung images.

This study contributes to lung cancer classification by proposing a modified CNN-based multiclass classification approach. Unlike previous studies that mainly focus on binary classification, this study addresses four distinct classes of lung nodule CT images, offering a more comprehensive representation of complex clinical needs. By modifying the VGG16 architecture with the addition of Flatten, Dense, and Dropout layers and applying the Softmax activation function, this approach enhances classification performance while reducing the risk of overfitting. The model is evaluated using five key metrics and compared with other popular CNN architectures, demonstrating the superiority of the proposed model. Furthermore, single-image prediction is tested as an initial step toward real-world application in diagnostic aid systems.

Although the VGG16 architecture has been widely applied in medical image classification, this study presents a distinct approach by specifically modifying its structure to improve multiclass lung nodule classification in CT images. The main contribution lies in integrating architectural modifications and training strategies designed to address challenges in complex medical image classification. The modification involves removing the default fully connected layer of VGG16 and adding new layers, including Flatten, two Dense layers with ReLU activation, Dropout, and Softmax. The addition of Dropout reduces the risk of overfitting [18] by randomly deactivating neurons during training, while ReLU improves the efficiency of the learning process. Additional experiments were conducted by replacing ReLU with LeakyReLU to mitigate the “dying ReLU” issue; however, the ablation study results showed no significant improvement over standard ReLU.

Preprocessing strategies used in this study, such as resizing images to 150×150 pixels and applying data augmentation through Keras’ ImageDataGenerator, effectively increased data variation and enhanced model robustness [19]. The novelty of this study lies not only in its technical modifications but also in its focus on multiclass classification—adenocarcinoma, large-carcinoma, normal, and squamous-carcinoma—which remains less explored than binary classification in lung cancer detection. Therefore, this study is expected to make a meaningful contribution to the development of computer-aided diagnosis (CAD) systems for more accurate and clinically applicable lung cancer detection.

TABLE 1
DISTRIBUTION OF LUNG CT SCAN IMAGES USED IN THE MODIFIED VGG16-CNN MODEL

CLASS	TRAIN	TEST	VALIDATION	TOTAL
ADENOCARCINOMA	275	79	39	393
LARGE-CARCINOMA	150	43	22	215
SQUAMOUS-CARCINOMA	123	35	18	176
NORMAL	146	40	26	212
TOTAL	694	197	105	996

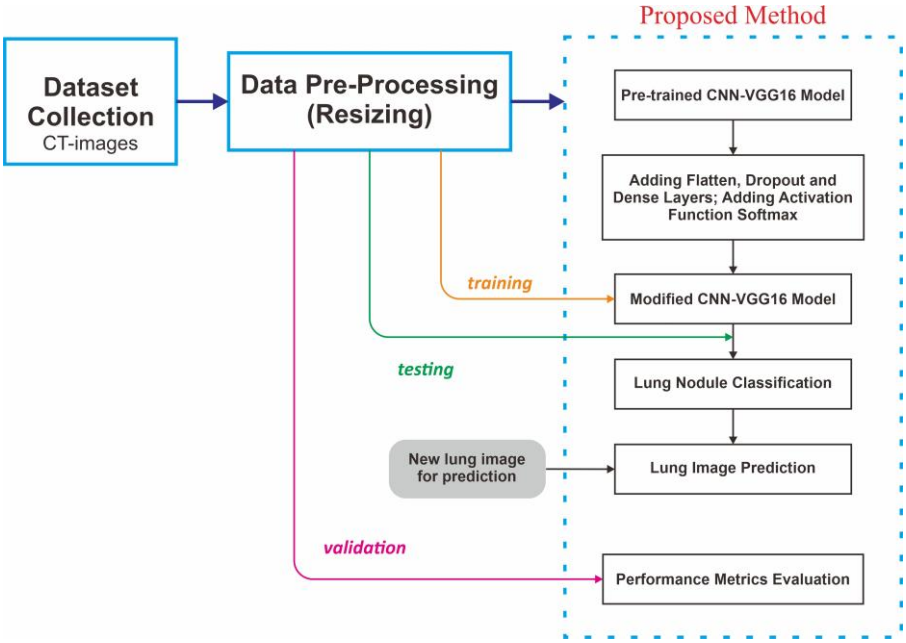

Figure 1. Methodology for lung nodule classification in CT images

II. RESEARCH METHOD

The methodology in this study consists of three stages: dataset collection, data preprocessing, and modification of the VGG16-CNN model architecture, as illustrated in Figure 1. The dataset was obtained from Kaggle and divided into three subsets: training, testing, and validation. The preprocessing stage involved resizing the images to ensure uniform input dimensions. The proposed model is a pre-trained VGG16-CNN architecture enhanced by adding Flatten, Dropout, and Dense layers, along with a Softmax activation function. After these modifications, the CNN-VGG16 model was trained using the training dataset (*data_train*). Once successfully trained, the model was tested using the testing dataset (*data_testing*) and validated using the validation dataset (*data_validation*). Finally, a single-image prediction test was conducted to evaluate the model's ability to classify an individual lung CT image into one of the learned classes.

A. Dataset Collection

This study uses a dataset of lung CT scan images obtained from a Kaggle project on chest cancer detection [20]. The dataset comprises 996 grayscale CT images in .jpg and .png formats, which have been preprocessed for compatibility with deep learning models. The data were compiled from multiple open-access sources by the dataset creator to support lung cancer subtype classification using convolutional neural networks (CNN). Unlike DICOM (DCM) files commonly used in clinical environments, these images were standardized into lightweight formats to enable faster training and simplified processing.

The dataset is organized into three primary folders—*train*, *test*, and *valid*—corresponding to 70%, 20%, and 10% of the data, respectively, as shown in Table 1. Each folder contains four subfolders representing different lung condition classes: Adenocarcinoma, Large-Carcinoma, Squamous-Carcinoma, and Normal (Healthy Lung Tissue).

Each class in the dataset exhibits distinct clinical characteristics that are crucial for accurate classification. Adenocarcinoma is the most common form of non-small cell lung cancer (NSCLC),

TABLE 2
ADDITION OF LAYERS IN THE MODIFIED VGG16-CNN MODEL

Layer (type)	Output Shape	Param #
flatten (Flatten)	(None, 8192)	0
dense (activation LeakyReLU)	(None, 100)	819300
dropout (Dropout)	(None, 100)	0
dense_1 (activation LeakyReLU)	(None, 50)	5050
dropout_1 (Dropout)	(None, 50)	0
dense_2 (activation Softmax)	(None, 4)	204
Total params:		824554
Trainable params:		824554
Non-trainable params:		0

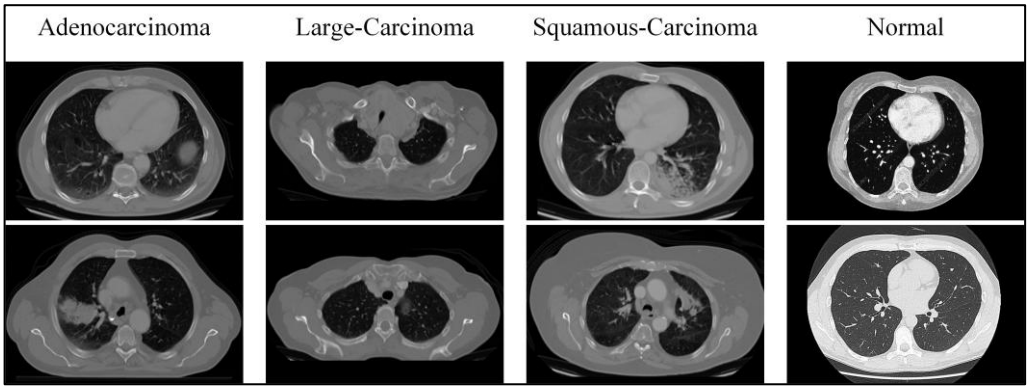

Figure 2. Four categories of lung CT image classes

typically originating in the mucus-producing glands located on the outer regions of the lungs. It accounts for approximately 40% of all NSCLC cases and is often associated with symptoms such as chronic cough and weight loss. Large-Carcinoma is an aggressive type of lung cancer that tends to grow and spread rapidly within the lungs. Although less common, it represents about 10–15% of NSCLC cases and generally requires more intensive treatment. Squamous-Carcinoma usually develops in the central part of the lungs, particularly in the bronchi (the main airways), and is strongly linked to smoking history. It constitutes roughly 30% of NSCLC cases. The Normal class includes CT scan images of healthy lungs with no nodules or visible abnormalities [20]. To enhance transparency and reproducibility, this study also presents visual examples of each class in Figure 2, showing the distinct visual characteristics learned by the model during training.

B. Preprocessing

The preprocessing stage in developing the lung CT image classification model involves several key steps. First, the dataset is organized into *data_train*, *data_testing*, and *data_validation* folders stored on Google Drive. The training process is conducted on Google Colaboratory by importing the dataset from Drive. The images are resized to 150×150 pixels using the *ImageDataGenerator* function from the Keras library to ensure uniformity across the training, testing, and validation datasets for the VGG16-CNN model. The dataset distribution follows a ratio of 70% for training, 20% for testing, and 10% for validation.

C. Modified VGG16-CNN Model

The base model used in this study for classifying lung CT images is the pre-trained VGG16 architecture, which was originally trained on the ImageNet dataset. Transfer learning was applied by excluding the fully connected layers of VGG16 and adding several new layers at the end of the architecture to perform the classification task, as illustrated in Table 2. The added layers include a Flatten layer, followed by two Dense layers with ReLU activation functions for feature extraction. A Dropout layer was also introduced to reduce overfitting [18], and a Softmax activation function was added to the output layer. The goal of these modifications is to develop a classification model with high accuracy and a low loss value, enabling the model to accurately classify multiclass lung CT images.

Table 2 presents the additional layers in the classification section, resulting in a total of 824,554 trainable parameters. The final layer uses a Softmax activation function with an output shape of 4,

$$f(Xc) = \frac{e^{Xc}}{\sum_j^c e^{xj}} \quad (1)$$

$$CE = -\sum_t^c (ti \log (f(x)\, i)) \quad (2)$$

$$Accuracy = \frac{TP + TN}{TP + TN + FP + FN} \text{ x } 100\% \quad (3)$$

$$Precision = \frac{TP}{TP + FP}\ x\ 100\% \quad (4)$$

$$Sensitivity = \frac{TP}{TP + FN}\ x\ 100\% \quad (5)$$

$$Specificity = \frac{TN}{FP + TN}\ x\ 100\% \quad (6)$$

$$F1 - Score = 2\ x\ \frac{Sensitivity\ x\ Precision}{Sensitivity + Precision}\ x\ 100\% \quad (7)$$

corresponding to the number of target classes. Softmax maps numerical outputs from the fully connected layer into class probabilities and is commonly used in networks for multiclass image classification tasks [21]. The Softmax function can be expressed as (1) and (2). In (1), *Xc* represents the output of the last fully connected layer, and *e* is the exponential constant. In (2), *C* denotes the total number of classes 4, and *t* represents the ground truth label or reference [22], corresponding to 0, 1, 2, and 3 for adenocarcinoma, large-carcinoma, normal, and squamous-carcinoma, respectively.

D. Training and Validation Process

After finalizing the model architecture and preparing the dataset, the next stage involved the training process. The training dataset consisted of 700 CT scan images of lung tissue representing four distinct classes. To adapt the pre-trained VGG16 architecture for multiclass classification, several modifications were made to its top layers. The original fully connected layers were removed and replaced with a Flatten layer, followed by two Dense layers with ReLU activation functions, a Dropout layer, and a final Dense layer with Softmax activation. The Flatten layer converts multidimensional feature maps into a one-dimensional vector suitable for input into fully connected layers [23]. The Dense layers function as feature decoders, learning complex, class-specific representations, while the Dropout layer randomly deactivates a portion of neurons during training to reduce overfitting [24]. This step is especially important given the moderate dataset size (996 images), which increases the risk of the model memorizing training data.

The model was compiled using the RMSprop optimizer, categorical cross-entropy as the loss function, and accuracy as the evaluation metric. Categorical cross-entropy is suitable for multiclass classification because it measures the difference between the predicted probability distribution and the true class labels. RMSprop was chosen for its ability to adapt the learning rate dynamically during training, making it effective for non-convex optimization problems such as deep CNNs [25]. Unlike standard stochastic gradient descent (SGD), RMSprop maintains an exponentially decaying average of squared gradients, allowing the model to converge faster and more stably on complex loss surfaces. Compared with optimizers like Adam, RMSprop often performs better for image classification tasks with small to medium-sized datasets, as it reduces oscillations that can occur with higher learning rates.

After training, the model was validated using a separate validation set consisting of 200 CT scan images. The resulting validation accuracy and loss values were used to evaluate how well the model generalized to unseen data. These metrics served as an initial measure of model robustness before proceeding to the final testing phase.

E. Testing and Evaluation

After completing the training process, the next stage involved testing the VGG16-CNN model for classifying lung cancer CT images. The testing used a dataset from the *test* folder consisting of 97 images. This step aimed to evaluate how accurately the proposed classification system could categorize lung cancer images into four classes. To assess the model's performance, several analytical parameters were used as benchmarks. Specifically, the Confusion Matrix was applied to determine the values of true positive (TP), true negative (TN), false positive (FP), and false negative (FN). TP represents predictions that correctly match the actual class, while TN refers to predictions correctly identified as non-target classes. FP indicates cases where the model incorrectly classified an image as positive, and FN refers to cases where the model failed to detect a positive instance [26]. The values obtained from the confusion matrix were used to calculate performance metrics, including accuracy (3), precision (4), sensitivity (5), specificity (6), and F1-score (7) [27].

To strengthen the reliability of the findings, each performance metric was complemented with a 95% confidence interval, estimated through a bootstrapping approach using 1,000 random resamplings of the test predictions. This method captures the variability and robustness of the model's performance, even when evaluated on a fixed test dataset. Confidence intervals provide a more informative interpretation of the results by indicating the expected range of variation if the experiment were replicated under similar conditions. This validation step ensures that the reported model performance is not only numerically strong but also statistically sound, reinforcing the effectiveness and reliability of the proposed modified VGG16-CNN model for multiclass classification of lung CT images.

F. The Image Prediction

Image prediction is the process of testing the VGG16-CNN model on a new, previously unseen image. A single image is used for this test, and the model classifies it into one of the learned categories. Among the four available classes, the model calculates the probability of similarity for each class in percentage form. The class with the highest predicted probability is selected as the final classification result.

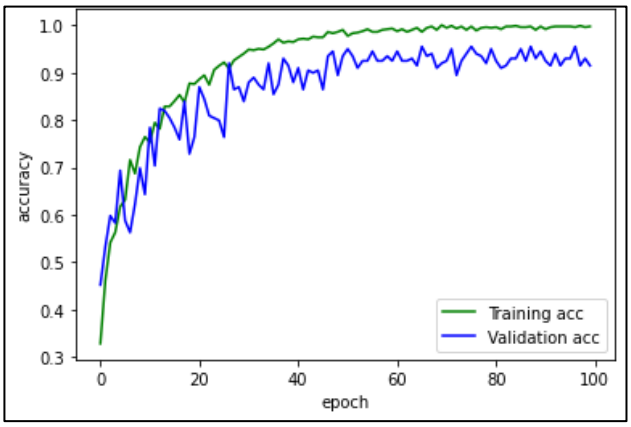

Figure 3. Training and validation accuracy graph of the modified VGG16-CNN model

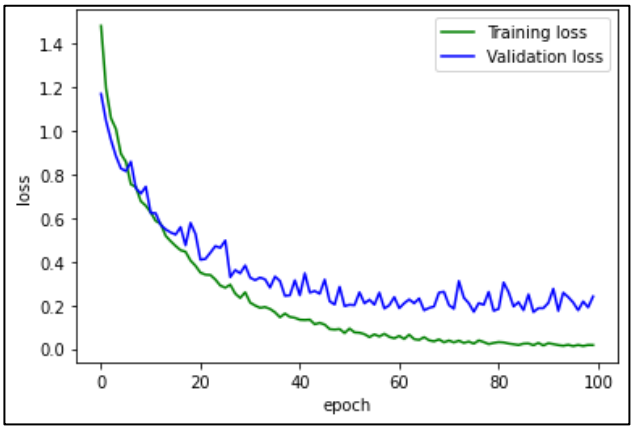

Figure 4. Training and validation loss graphs of the modified VGG16-CNN model

III. Results and Discussion

The training and validation accuracy of the modified VGG16-CNN model is illustrated in Figure 3. The model demonstrates a steady increase in accuracy as the number of epochs rises, indicating effective learning from the CT scan image data. Similarly, the validation accuracy improves in parallel, suggesting that the model generalizes well without signs of overfitting during training.

The accuracy graph in Figure 3 plots accuracy values against epoch values, with epochs represented on the x-axis and accuracy on the y-axis. When trained for 100 epochs, the accuracy increases consistently as the number of epochs grows. This upward trend demonstrates that the modified VGG16-CNN model effectively learns from lung CT scan image data. Likewise, validation accuracy shows a similar increasing pattern, confirming that the model performs well in classifying lung CT scan images.

Figure 4 illustrates the training and validation loss curves, both showing a consistent decline as training progresses. The gradual reduction in loss values without abrupt fluctuations indicates stable convergence of the model. In the graph, epochs are shown on the x-axis and loss values on the y-axis. The decreasing loss trend reflects that the model trains effectively and avoids overfitting. Consequently, based on the training and validation loss graphs, the modified VGG16-CNN model demonstrates high accuracy and strong performance in lung image classification.

Figure 5 presents the confusion matrix, which illustrates the model's performance in classifying lung CT scan images into four categories: adenocarcinoma, large-carcinoma, normal, and squamous-carcinoma. The x-axis represents the predicted labels for the four classes, while the y-axis represents the actual labels. The darker diagonal boxes in the confusion matrix indicate the number of correctly predicted images that match the actual data. The matrix includes values for true positives, true negatives, false positives, and false negatives, allowing assessment of the model's classification ability in terms of accuracy, precision, and sensitivity. The clear diagonal dominance indicates that most predictions align with the ground truth labels, confirming the model's strong classification performance. Based on the confusion matrix, key evaluation metrics—accuracy (90.72%), precision (91.50%), sensitivity (89.25%), specificity (96.76%), and F1-score (90.00%)—were computed and summarized in Table 3.

Table 3
Performance Metrics of the Modified VGG16-CNN Model

CNN Architecture	Performance Metrics					
	Accuracy (%)	Precision (%)	Sensitivity (%)	Specificity (%)	F1-Score (%)	Loss
Modified VGG-16 CNN	90.72	91.50	89.25	96.76	90.00	0.37
EfficientNetB1	89.69	90.50	90.00	96.44	84.75	1.02
MobileNetV2	84.54	87.50	83.75	94.52	90.00	1.22
AlexNet	72.16	19.75	19.75	73.36	19.25	2.02
ResNet50	58.76	74.00	54.00	85.84	55.50	1.07

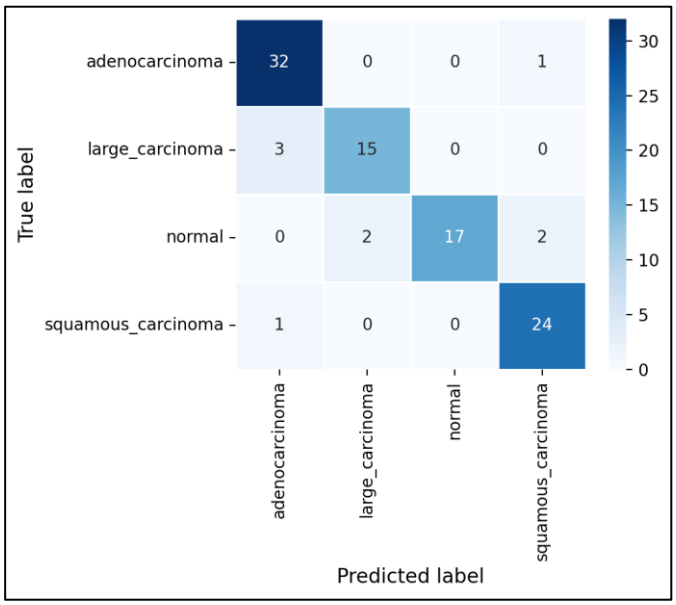

Figure 5. Confusion matrix of the modified VGG16-CNN model

A comparative analysis was also performed with several established CNN architectures: AlexNet, MobileNetV2, EfficientNetB1, and ResNet50. As shown in Table 3, the modified VGG16-CNN outperformed all other models across every evaluation metric. This improvement can be attributed to architectural enhancements, including the removal of default fully connected layers and the addition of customized layers such as Flatten, Dense layers with ReLU activation functions, Dropout for regularization, and Softmax for multiclass prediction. These modifications enhanced feature generalization while maintaining a compact model size. In addition, resizing images to 150×150 pixels and applying data augmentation improved variability during training, contributing to greater model robustness.

Accuracy, loss, sensitivity, precision, specificity, and F1-score of the Modified VGG16-CNN are summarized in Table 2. A comparative analysis was also performed using other CNN architectures, including AlexNet, MobileNetV2, EfficientNetB1, and ResNet50. The purpose of this comparison is to evaluate how well the Modified VGG16-CNN performs in multiclass lung cancer CT image classification. The Modified VGG16-CNN shows better performance than the other architectures based on the parameters used in this study. It achieved an accuracy of 90.72%, a precision of 91.50%, a sensitivity of 89.25%, a specificity of 96.76%, an F1-score of 90%, and a low loss of 0.37. The use of a classification layer and automatic feature extraction optimizes the neural network's ability to recognize objects in images. The convolution, pooling, fully connected, flatten, dense, dropout, and Softmax operations contribute to strong object recognition and enable classification with low loss as well as high accuracy, sensitivity, specificity, precision, and F1-score.

Compared with ResNet50 and EfficientNetB1, which have deeper and more complex architectures, the Modified VGG16-CNN reaches higher performance with lower computational cost. This result may be related to its better suitability for small medical imaging datasets. EfficientNetB1 produced competitive accuracy (89.69%) but had a higher loss value (1.02), indicating less stable optimization. ResNet50, although widely used in many classification tasks, performed poorly in this study (accuracy 58.76%), which may be due to overfitting or difficulty in converging on limited data. AlexNet also produced low performance, with an F1-score of 19.25%. This is likely due to its shallow architecture and limited capacity to extract complex features needed to distinguish subtle differences among multiple lung cancer subtypes.

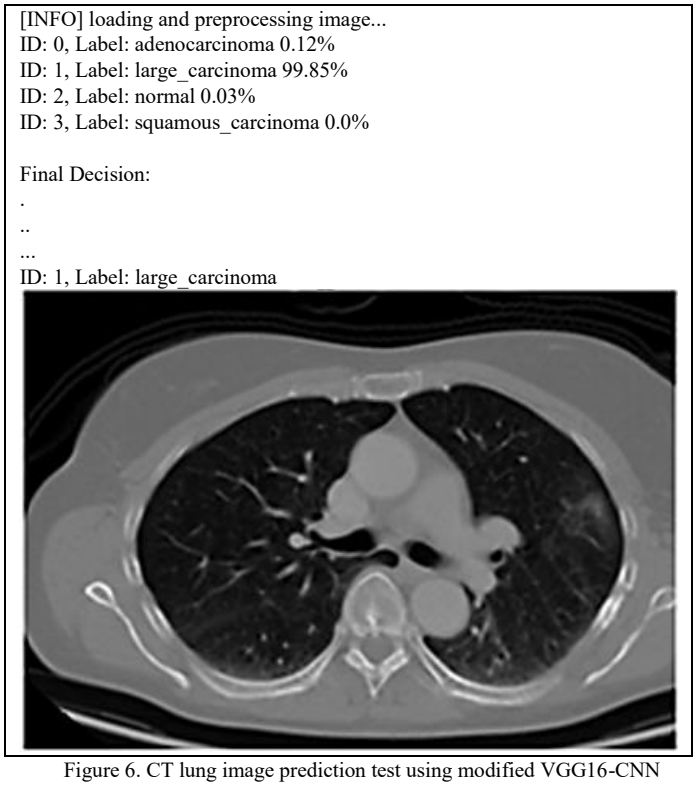

Figure 6. CT lung image prediction test using modified VGG16-CNN

Despite the strong performance, the Modified VGG16-CNN model has several limitations. The model was effective in distinguishing four lung cancer classes, but its performance may decrease with larger datasets or additional classes because of its relatively shallow architecture. Although Dropout was applied to reduce overfitting, further improvements could be achieved by exploring other regularization methods such as batch normalization or more advanced data augmentation strategies. ReLU was selected for simplicity and efficiency, and the ablation study showed no meaningful improvement when replaced with LeakyReLU, although additional investigation using larger datasets may provide different results.

Recent studies have also shown increased interest in deep learning for lung cancer classification. Chiet et al. (2024) proposed a pre-trained VGG16 method by adding several fully connected layers to classify three-class lung cancer CT images and achieved an accuracy of 86.71% [28]. These findings highlight the importance of architectural design and preprocessing strategies for multiclass CT image classification. In this context, the modified VGG16 used in this study represents a lightweight but effective alternative with competitive performance and lower training complexity.

A prediction test using a single image was conducted to simulate real-world deployment. As shown in Figure 6, the model successfully classified a large-carcinoma image with a confidence level of 99.85%, indicating its potential usefulness in clinical decision support systems.

IV. CONCLUSION

The modified VGG16-CNN architecture for classifying lung nodules demonstrates strong performance and has promising potential for future clinical application. In this study, the model classified CT images of lung nodules into four classes: adenocarcinoma, large carcinoma, squamous carcinoma, and normal. The model achieved an accuracy of 90.72 percent, indicating that it can correctly classify most images. The precision of 91.5 percent reflects the high level of reliability in identifying positive cases. The sensitivity of 89.25 percent shows the model's ability to correctly detect images with positive characteristics, while the specificity of 96.76 percent indicates the likelihood of correctly identifying images without the characteristics of lung cancer. In addition, the model achieved an F1-score of 90 percent and a low loss value of 0.37. The modified VGG16-CNN model was compared with several other CNN architectures, including ResNet50, EfficientNetB1, MobileNetV2, and AlexNet. This comparison aimed to evaluate performance in multiclass lung cancer CT image classification. The results confirm that the modified VGG16-CNN provides superior performance and is capable of accurately classifying lung CT scan images into four categories. This study shows that the proposed approach is effective in diagnosing lung nodules from CT images. The model has the potential to assist medical professionals in making accurate and timely diagnostic decisions, which may help prevent delays in patient care and treatment.

Although this study achieved good results in classifying lung cancer, it still has several limitations. The model was trained and tested on one dataset with limited diversity and image quantity, so applying it to other datasets may lead to different results. Limited computing resources also affected the experiment, since more powerful hardware would allow faster training and improved model performance. This study has also not been tested in real-world clinical settings. For future improvements, expanding the training dataset is needed because CNN models perform better when trained on a larger volume of images. Increasing the number of samples will help the model learn image features in each class more effectively. It is also important to incorporate additional lung cancer types to increase class representation. Applying enhanced preprocessing techniques may further improve feature visibility and classification performance. In addition, testing the model in clinical environments is essential so that it can support radiologists in early lung cancer detection.

REFERENCES

[1] H. Jiang, H. Ma, W. Qian, M. Gao, and Y. Li, "An Automatic Detection System of Lung Nodule Based on Multigroup Patch-Based Deep Learning Network," *IEEE J. Biomed. Heal. Informatics*, vol. 22, no. 4, pp. 1227–1237, 2018, doi: 10.1109/JBHI.2017.2725903.

[2] R. L. Siegel, K. D. Miller, H. E. Fuchs, and A. Jemal, "Cancer statistics, 2022," *CA. Cancer J. Clin.*, vol. 72, no. 1, pp. 7–33, 2022, doi: 10.3322/caac.21708.

[3] S. Kido, Y. Hirano, and N. Hashimoto, "Detection and classification of lung abnormalities by use of convolutional neural network (CNN) and regions with CNN features (R-CNN)," *2018 Int. Work. Adv. Image Technol. IWAIT 2018*, pp. 1–4, 2018, doi: 10.1109/IWAIT.2018.8369798.

[4] S. Sari, T. Sutikno, I. Soesanti, and N. A. Setiawan, "A review of convolutional neural network-based computer-aided lung nodule detection system," *IAES Int. J. Artif. Intell.*, vol. 12, no. 3, pp. 1044–1061, 2023, doi: 10.11591/ijai.v12.i3.pp1044-1061.
[5] Y. Chen, X. Duan, S. Chatani, W. Du, J. Wang, and Q. Hu, "An Improved Region-based Fully Convolutional Network for Automatic Pulmonary Nodules Detection," pp. 256–261, 2019.
[6] A. Agarwal, K. Patni, and D. Rajeswari, "Lung Cancer Detection and Classification Based on Alexnet CNN," *Proc. 6th Int. Conf. Commun. Electron. Syst. ICCES 2021*, pp. 1390–1397, 2021, doi: 10.1109/ICCES51350.2021.9489033.
[7] F. William, A. Serener, and S. Serte, "Deep learning classification of Covid-19, pneumonia, and lung cancer on chest radiographs," *ISMSIT 2021 - 5th Int. Symp. Multidiscip. Stud. Innov. Technol. Proc.*, pp. 125–129, 2021, doi: 10.1109/ISMSIT52890.2021.9604629.
[8] N. Jahan, M. S. Anower, and R. Hassan, "Automated Diagnosis of Pneumonia from Classification of Chest X-Ray im ages using EfficientNet," *2021 Int. Conf. Inf. Commun. Technol. Sustain. Dev. ICICT4SD 2021 - Proc.*, pp. 235–239, 2021, doi: 10.1109/ICICT4SD50815.2021.9397055.
[9] M. Yaqoob, H. Qayoom, and F. Hassan, "Covid-19 Detection Based on the Fine-Tuned MobileNetv2 Through Lung X-rays," *2021 4th Int. Symp. Adv. Electr. Commun. Technol.*, pp. 01–06, 2022, doi: 10.1109/isaect53699.2021.9668425.
[10] N. Y. Wu *et al.*, "Magnetic resonance imaging for lung cancer detection: Experience in a population of more than 10,000 healthy individuals," *BMC Cancer*, vol. 11, 2011, doi: 10.1186/1471-2407-11-242.
[11] R. Zhang, C. Cheng, X. Zhao, and X. Li, "Multiscale Mask R-CNN–Based Lung Tumor Detection Using PET Imaging," *Mol. Imaging*, vol. 18, pp. 1–8, 2019, doi: 10.1177/1536012119863531.
[12] T. Messay, R. C. Hardie, and T. R. Tuinstra, "Segmentation of pulmonary nodules in computed tomography using a regression neural network approach and its application to the Lung Image Database Consortium and Image Database Resource Initiative dataset," *Med. Image Anal.*, vol. 22, no. 1, pp. 48–62, 2015, doi: 10.1016/j.media.2015.02.002.
[13] H. Shi, Z. Peng, and H. Wan, "Pulmonary Nodules Detection Based on CNN Multi-scale Feature Fusion," *2019 IEEE 11th Int. Conf. Adv. Infocomm Technol. ICAIT 2019*, pp. 86–90, 2019, doi: 10.1109/ICAIT.2019.8935936.
[14] S. Pang *et al.*, "VGG16-T: A novel deep convolutional neural network with boosting to identify pathological type of lung cancer in early stage by ct images," *Int. J. Comput. Intell. Syst.*, vol. 13, no. 1, pp. 771–780, 2020, doi: 10.2991/ijcis.d.200608.001.
[15] G. K. Abraham, P. Bhaskaran, and V. S. Jayanthi, "Lung nodule classification in CT images using convolutional neural network," *Proc. 2019 9th Int. Conf. Adv. Comput. Commun. ICACC 2019*, pp. 199–203, 2019, doi: 10.1109/ICACC48162.2019.8986213.
[16] N. Akter, M. T. Reza, and M. A. Alam, "A Comparison Based Analysis on the Performance of Deep Neural Network Models in Terms of Classifying Pneumonia from Chest X-ray Images," *2020 IEEE Asia-Pacific Conf. Comput. Sci. Data Eng. CSDE 2020*, 2020, doi: 10.1109/CSDE50874.2020.9411560.
[17] A. Y. Saleh, C. K. Chin, V. Penshie, and H. R. H. Al-Absi, "Lung cancer medical images classification using hybrid cnn-svm," *Int. J. Adv. Intell. Informatics*, vol. 7, no. 2, pp. 151–162, 2021, doi: 10.26555/ijain.v7i2.317.
[18] N. Srivastava, G. Hinton, A. Krizhevsky, I. Sutskever, and R. Salakhutdinov, "Dropout : A Simple Way to Prevent Neural Networks from Overfitting," *J. Mach. Learn. Res.*, vol. 15, pp. 1929–1958, 2014.
[19] S. Hossain, N. Basak, A. Mollah, Nahiduzzaman, M. Ahsan, and J. Haider, "Ensemble-based multiclass lung cancer classification using hybrid CNN-SVD feature extraction and selection method," pp. 1–30, 2025, doi: 10.1371/journal.pone.0318219.
[20] M. Hany, "Chest CT-Scan images Dataset." Accessed: Mar. 24, 2024. [Online]. Available: https://www.kaggle.com/mohamedhanyyy/chest-ctscan-images
[21] N. D. Miranda, L. Novamizanti, and S. Rizal, "Convolutional Neural Network Pada Klasifikasi Sidik Jari Menggunakan Resnet-50," *J. Tek. Inform.*, vol. 1, no. 2, pp. 61–68, 2020.
[22] N. Yudistira, A. W. Widodo, and B. Rahayudi, "Deteksi Covid-19 Pada Citra Sinar-X Dada Menggunakan Deep Covid-19 Detection on X-Ray Images Using Efficient Deep Learning," *J. Teknol. Inf. dan Ilmu Komput.*, vol. 7, no. 6, pp. 1289–1296, 2020, doi: 10.25126/jtiik.202073651.
[23] S. Dodia, A. B., and P. A. Mahesh, "Recent advancements in deep learning based lung cancer detection: A systematic review," *Eng. Appl. Artif. Intell.*, vol. 116, 2022, doi: https://doi.org/10.1016/j.engappai.2022.105490.
[24] M. M. Ansari *et al.*, "Evaluating CNN Architectures and Hyperparameter Tuning for Enhanced Lung Cancer Detection Using Transfer Learning," *J. Electr. Comput. Eng.*, vol. 2024, 2024, doi: 10.1155/2024/3790617.
[25] Y. N. Dauphin, H. De Vries, J. Chung, and Y. Bengio, "RMSProp and equilibrated adaptive learning rates for non-convex optimization," 2014.
[26] S. Sasikala, M. Bharathi, and B. R. Sowmiya, "Lung Cancer Detection and Classification Using Deep CNN," *Int. J. Innov. Technol. Explor. Eng.*, vol. 8, no. 2, pp. 259–262, 2018.
[27] P. N. Andono, T. Sutojo, and Muljono, "Pengolahan Citra Digital." [Online]. Available: https://books.google.co.id/books?id=zUJRDwAAQBAJ&printsec=frontcover&hl=id&source=gbs_ge_summary_r&cad=0#v=onepage&q&f=false
[28] C. C. Chiet, K. W. How, P. Y. Han, and Y. H. Yen, "A Lung Cancer Detection With Pre - Trained CNN Models," *J. Informatics Web Eng.*, vol. 3, no. 1, 2024.